Progress In Electromagnetics Research B, Vol. 51, 291–306, 2013

ANALYSIS OF ELECTROMAGNETIC FIELD COUPLING TO MICROSTRIP LINE CONNECTED WITH NONLINEAR COMPONENTS

Hui Yan[1], Liping Yan[1, *], Xiang Zhao[1], Haijing Zhou[2], and Kama Huang[1]

[1]School of Electronics and Information Engineering, Sichuan University, Chengdu 610064, China

[2]Institute of Applied Physics and Computation Mathematics, Beijing 100088, China

Abstract—An analysis method for electromagnetic field coupling to microstrip line connected with nonlinear components is proposed in this paper. Different from the published work, not only the voltage and current response of the nonlinear component connected to the transmission line (TL) can be obtained, but also the power transmitted from this nonlinear component to the next one at both the fundamental frequency and harmonics can be predicted. The proposed method suitably combines the classical field-to-TL coupling theory and the nonlinear large-signal scattering parameters on the basis of a black box model in frequency-domain. Then this method is experimentally validated by a laboratory system including a microstrip line connected with a simple nonlinear component constituted by the anti-paralleled HSMS-282C Schottky diodes pair welded to a 50 Ω microstrip line. The calculated results using the proposed method show good agreement with the measured data.

1. INTRODUCTION

The electromagnetic environmental effects attract increasing interests of researchers and engineers as more and more wireless communication systems have been developed and applied widely. In recent years, researchers begin to pay increasing attentions to electromagnetic compatibility analysis on system level [1, 2]. The electromagnetic compatibility modeling inside an electronic system involves several

Received 20 March 2013, Accepted 25 April 2013, Scheduled 29 April 2013

* Corresponding author: Liping Yan (sherryyan05@gmail.com).

big problems, such as aperture coupling, field-to-transmission line (TL) coupling, nonlinear components modeling which is necessary for circuit simulation. External electromagnetic wave can penetrate into the system through apertures or slots, and then induce current on TLs. This induced current may flow along the wires and elements in the system and cause interference. Though we can use powerful commercial software like ADS and HSPICE to simulate circuits and calculate the voltage or current on each element, it is hard to set up the electromagnetic compatibility model of the whole system illuminated by electromagnetic waves. One of the challenges is the evaluation of electromagnetic field coupling to TL connected with a nonlinear component and the prediction of the transmitted power from this nonlinear component towards the next element/device.

Classical field-to-TL coupling theory has been developed and frequently used to compute the coupling of electromagnetic fields to TLs with linear terminations [3–14]. Especially, the radiated interference on printed circuit board (PCB) layout through the field-to-TL route has become a growing concern in prediction of system reliability [15, 16]. However, nonlinear electronic components or devices are essential parts of electronic systems. It is hard to analyze the electromagnetic field coupling to TLs connected with nonlinear loads since the response of the nonlinear loads is more complicated than of linear ones. Several approaches have been developed to try to solve this problem. Tesche provided an example to illustrate the application of transient BLT equation, which is first proposed in 1999 [17], to the external electromagnetic field coupling to a TL with nonlinear termination [18, 19]. However, it is not convenient to use for nonlinear loads where a nonlinear matrix equation should be solved first to determine the reflection coefficients in time domain [20]. The effects of nonlinear termination on the multi-transmission line in time-domain are also investigated using finite-difference time-domain (FDTD) method for dynamic nonlinear elements [21]. As we all know, large computational consumption is needed to solve such a problem using full wave analysis. Xie proposed a hybrid FDTD-SPICE method [22] to analyze lossless TLs with nonlinear or time-varying loads illuminated by a non-uniform electromagnetic, in which effective voltage and current sources are obtained first using field-to-TL coupling method after the incident fields to the lines are calculated using FDTD, and then imported into SPICE to deal with the nonlinear loads [23]. Bayram mentioned nonlinear loads in the hybrid S-parameters method used for field-to-TL coupling [24], but again the nonlinear loads had to be handled by HSPICE or ADS.

In these methods mentioned above, nonlinear components are

handled as the terminal loads of the TL, namely, a one-port network. However, in the real electronic system, nonlinear components or devices sometimes connect with other components or TLs, working as two-port or multi-port networks. How to model such a system and get the output power from the nonlinear components is still a big challenge. It is often too complex to permit complete EMC simulation at the device level of description. A complete system simulation can become practical, however, provided that the models of the nonlinear blocks or ICs are given [25]. Therefore, a more applicable model, which can be combined conveniently with field-to-TL coupling theory and S-parameters of linear components, is necessary for nonlinear components. Though the nonlinear large-signal scattering parameters based on the black box model in frequency-domain [26] can be used to model nonlinear networks, much efforts are necessary to combine this model with field-to-TL coupling theory properly.

The goal of this paper is to develop an analysis method for electromagnetic field coupling to microstrip line connected with nonlinear components and then obtain the output power from this nonlinear component towards the next element. The proposed method builds upon the classical field-to-TL coupling theory and nonlinear large-signal scattering parameters, and skills for combination of these two models are considered. In the following, the complete analysis method is presented in Section 2. The predicted results from the proposed method and experimental validation are provided in detail in Section 3 and we summarize our work briefly in Section 4.

2. MODELS AND BASIC PRINCIPLES

The classical field-to-TL coupling model is usually applied to calculate the voltage and current induced along the line or on linear loads. If a nonlinear component is connected to the line not as a termination, as a result, the output from the nonlinear component will influence the response of the next component. In order to analyze such a case, the nonlinear large-signal scattering parameters based on the black box model in frequency-domain are used to describe the nonlinear component or devices. With this model, whatever the nonlinear component, device and even subsystem are, all can be described concisely by a scattering parameters matrix [27].

2.1. Field-to-transmission Line Coupling Theory

Microstrip lines are taken into consideration here due to their popular applications in microwave system. Fig. 1 shows such a line illuminated

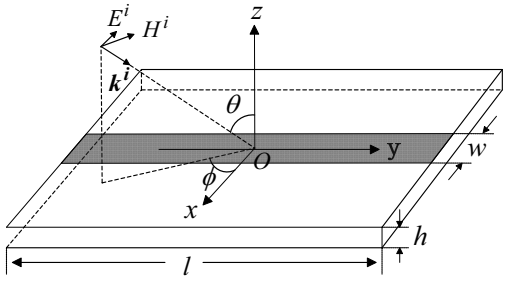

Figure 1. Microstrip structure illuminated by electromagnetic wave.

by a time-harmonic electromagnetic wave with frequency ω.

Three models proposed by Taylor, Agrawal and Rachidi respectively all can be used to describe the field interaction with TLs, and the total induced voltage waveforms obtained using them are identical [28–30]. The Taylor model is used here, because the total current and voltage induced on the line are expected in order to get the response of the linear/nonlinear component connected with the line. The external field results in a forcing function expressed in terms of the exciting magnetic and electric flux. This forcing function (source terms) are included as a set of distributed series voltage and parallel current sources along the line. Consequently, the TL equations are described as (1a) and (1b).

$$\frac{dV(y)}{dy} + j\omega LI(y) = v_s(y) \tag{1a}$$

$$\frac{dI(y)}{dy} + j\omega CV(y) = i_s(y) \tag{1b}$$

where the distributed voltage and current source excitation terms v_s and i_s for the microstrip line structure can be written as (2a) and (2b), and the per-unit-length inductance L and capacitance C are defined as (3a) and (3b) [31].

$$v_s(y) = j\omega\mu_0 \int_0^h H_x^p(0,y,z)dz \tag{2a}$$

$$i_s(y) = -j\omega C \int_0^h E_z^p(0,y,z)dz + j\omega\varepsilon_1 \int_{-w/2}^{w/2} E_z^p(x,y,h)dx \tag{2b}$$

$$L = \frac{-\int_0^h \mu_0 \mathbf{H}^s(0,y,z)\cdot\hat{x}dz}{\int_{-w/2}^{+w/2} \mathbf{J}_s(x,y)\cdot\hat{y}dx} \tag{3a}$$

$$C = \frac{\int_{-w/2}^{+w/2} \varepsilon_1 \mathbf{E}^s(x,y,h)\cdot\hat{z}dx}{\int_0^h \mathbf{E}^s(0,y,z)\cdot\hat{z}dz} \tag{3b}$$

where the "primary" fields ($\mathbf{E}^p$, $\mathbf{H}^p$) are defined as the field excited by the incident electromagnetic wave in the presence of the ground plane and the dielectric substrate and in the absence of the metal strip. The "secondary" fields ($\mathbf{E}^s$, $\mathbf{H}^s$) are the field scattered by the microstrip conductor when excited by the "primary" field and in the presence of the ground plane and the dielectric substrate.

Note that the TL approximation (or the quasi-TEM assumption) is used in these filed-to-TL coupling models. This approximation is mainly limited by the condition that the transverse dimensions of the line and its return path (essentially the line height) should be much smaller than the minimum significant wavelength of the exciting electromagnetic field $\lambda_{\min}$, which corresponds to a cutoff frequency. Beyond that, higher modes may be excited and the classical models are not suitable for such a problem. As a result, the high-frequency field-to-TL coupling theory should be used [28]. This, however, is beyond the scope of this paper.

2.2. Nonlinear Components Modeling

The nonlinear large-signal scattering parameters, which are based on the black box model in frequency-domain, are used to describe the characteristics of nonlinear devices or circuits [26]. Nonlinear large-signal S-parameters can be defined as ratios of the reflected and incident wave variables of each port [32], including the fundamental and harmonic components of the input and output signals since energy can be transferred to other frequencies in a nonlinear device. Note that the nonlinear S-parameters can be used to describe any nonlinear N-port network. If harmonic components up to mth order are taken into consideration, the nonlinear S-parameters will be a $(N \times m)^2$ matrix. In this paper, for the nonlinear component used in the following experiments, the power of harmonics greater than 3rd are much less than that of the third harmonic and can be neglected. Therefore, a two-port network with harmonics up to 3rd, as shown in Fig. 2, is

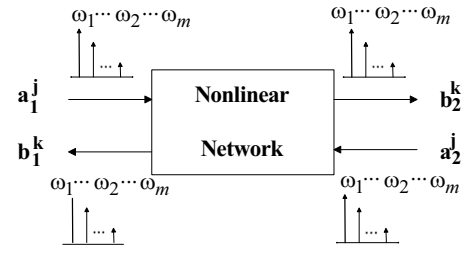

Figure 2. Diagram of a nonlinear two-port network.

considered as an example.

In Fig. 2, a_m^j and b_n^k represent the incident and reflected travelling waves, where the subscripts m and n denote the port number and superscripts j and k denote the spectral component number, respectively. Based on the S-parameters defined for a linear network, let if only the fundamental, second and third harmonic components are taken into account, nonlinear **S**-matrix is given in the following equation,

$$\begin{bmatrix} b_1^1 \\ b_1^2 \\ b_1^3 \\ \hline b_2^1 \\ b_2^2 \\ b_2^3 \end{bmatrix} = \left[\begin{array}{ccc:ccc} S_{11}^{11} & S_{11}^{12} & S_{11}^{13} & S_{12}^{11} & S_{12}^{12} & S_{12}^{13} \\ S_{11}^{21} & S_{11}^{22} & S_{11}^{23} & S_{12}^{21} & S_{12}^{22} & S_{12}^{23} \\ S_{11}^{31} & S_{11}^{32} & S_{11}^{33} & S_{12}^{31} & S_{12}^{32} & S_{12}^{33} \\ \hline S_{21}^{11} & S_{21}^{12} & S_{21}^{13} & S_{22}^{11} & S_{22}^{12} & S_{22}^{13} \\ S_{21}^{21} & S_{21}^{22} & S_{21}^{23} & S_{22}^{21} & S_{22}^{22} & S_{22}^{23} \\ S_{21}^{31} & S_{21}^{32} & S_{21}^{33} & S_{22}^{31} & S_{22}^{32} & S_{22}^{33} \end{array}\right] = \begin{bmatrix} a_1^1 \\ a_1^2 \\ a_1^3 \\ \hline a_2^1 \\ a_2^2 \\ a_2^3 \end{bmatrix} \tag{4}$$

where each element S_{nm}^{kj} in [**S**] can be defined as

$$S_{nm}^{kj} = \frac{b_n^k}{a_m^j} \begin{cases} a_x^y = 0 & \text{for } x \neq m \\ a_x^y = 0 & \text{for all } x = m \ \& \ \text{all } y \neq j \end{cases} \tag{5}$$

Figure 3 shows a flow chart to illustrate the mechanism of the proposed method in detail. First the induced voltage and current along the line are calculated using the field-to-TL coupling theory. If a nonlinear component is connected to the line, the equivalent impedance Z_{eff} should be obtained in advance in order to solve the TL equations, because it varies in terms of the power input to the nonlinear component. As a result, the induced voltage and current along the line change accordingly. That will be discussed in detail later.

Based on the induced voltage and equivalent impedance, the power of the incident wave to the nonlinear component is achieved. Then the nonlinear S-parameters of the nonlinear components are extracted by experiments. Based on these S-parameters and power of the incident wave, the output power from the nonlinear component can be predicted. Note that the nonlinear S-parameters based on the black-box model can describe any nonlinear elements or devices. Consequently, the proposed method has a good applicability as long as the necessary S-parameters of nonlinear components/devices are known. An example for extraction of nonlinear S-parameters using experiments is described in the following.

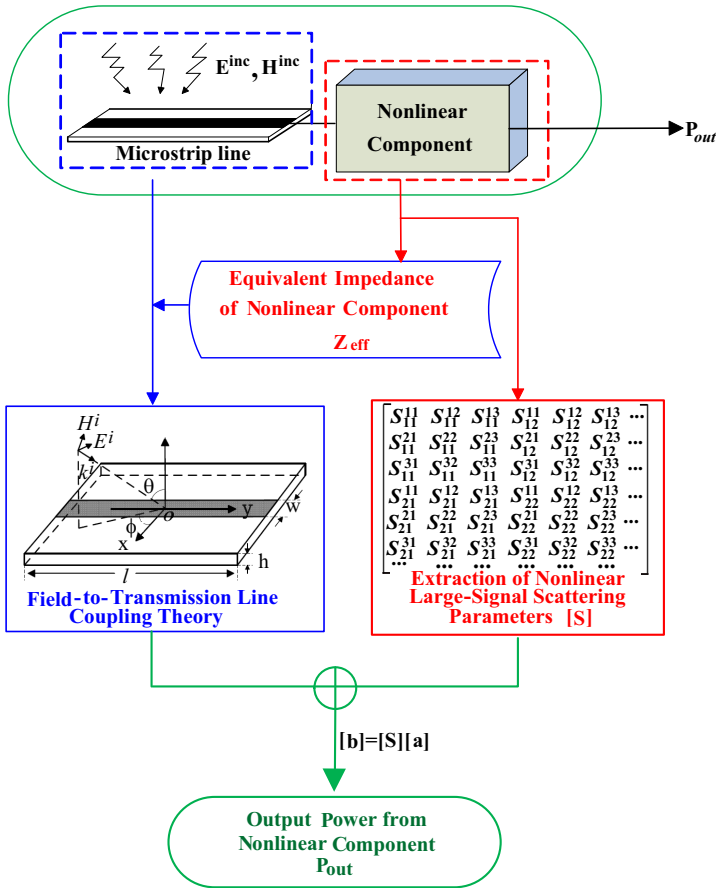

Figure 3. The flow chart of the proposed method.

2.3. Extraction of Nonlinear Large-signal Scattering Parameters

In this part, an example is presented to show how to extract the nonlinear S-parameters. Fig. 4 provides a simple nonlinear component

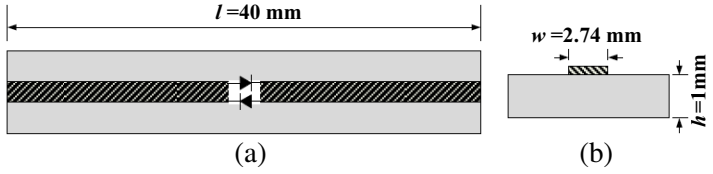

Figure 4. The nonlinear component under test, (a) top view and (b) side view.

consists of an anti-paralleled HSMS-282C Schottky diodes pair welded at the center of the conductor strip of a 50 Ω microstrip line printed on a 1 mm thick substrate with relative dielectric constant $\varepsilon_r = 2.65$. Several significant parameters in **S**-matrix of the nonlinear component are extracted through measurements. The block diagram and the photograph of the real experimental system are depicted in Fig. 5.

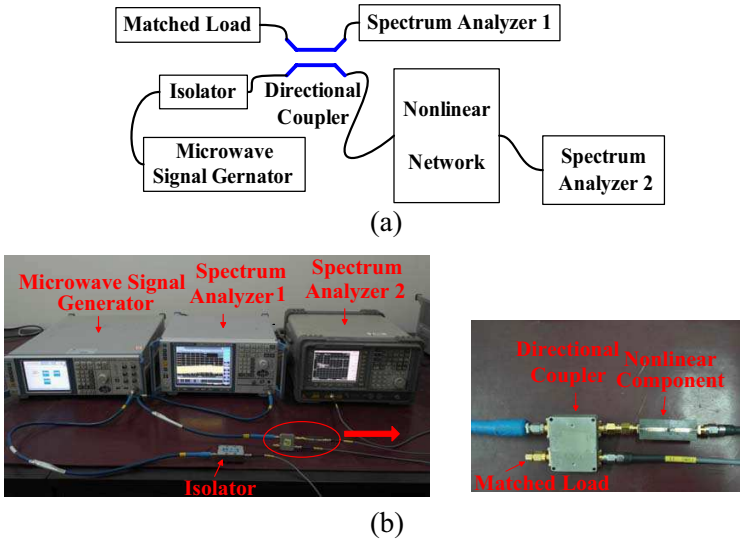

Figure 5. (a) Block diagram and (b) photograph of the experimental system.

A single-tone signal at frequency 2.5 GHz excites the nonlinear component, and the power of reflected and transmitted waves are measured using two broadband spectrum analyzers ($\sim$ 26.5 GHz) respectively. The transmitted power is measured directly, while the reflected wave is sent to the spectrum analyzer through a directional coupler with coupling of 20 dB, and it makes the measurement difficult if the reflected power is very small. The power of the fundamental and harmonic components in the reflected and transmitted waves is measured as the input power varies from −5 dBm to 18 dBm gradually. The amplitudes of four parameters in **S**-matrix are extracted and results are given in Fig. 6.

Those measured results include only the fundamental and the third harmonic components, while the second harmonic component cannot be detected because the even harmonic components circulate within the loop formed by the two anti-paralleled diodes [33]. Although fifth harmonic can also be observed on spectrum analyzer but its power

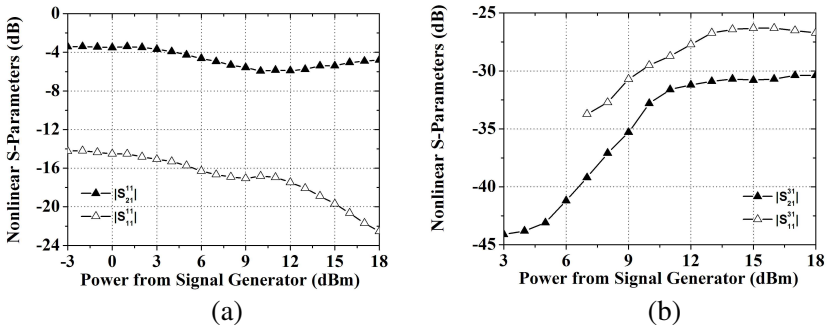

Figure 6. Measured nonlinear S-parameters: (a) the fundamental and (b) the third harmonic components.

is far less than the third harmonic. The reflection and transmission of both the fundamental and third harmonic components vary nonlinearly in terms of the input power in Fig. 6. Especially, the power of the fundamental component is much larger than that of the third harmonic ones. For further inspection of Fig. 6, the transmitted power is larger than the reflected one for the fundamental component, but just the opposite for the third harmonic. Here the reflected power of the third harmonic component can be detected only when the input power is greater than 7 dBm, because the reflected wave is attenuated by 20 dB due to the directional coupler before measured using spectrum analyzer.

Using the field-to-TL coupling model mentioned previously, the voltage and current induced along the microstrip line can be obtained and then the power transmitted to the component connected with the line can be calculated. Combined with the nonlinear large-signal S-parameters, we can predict the output power of fundamental and harmonic components from the nonlinear component towards the next element.

3. RESULTS AND ANALYSIS

The validation of the results obtained from the proposed analysis method is supported by experimental data measured on a laboratory system, as shown in Fig. 7. A TEM cell is used to generate a relatively uniform electromagnetic field, and a 40 mm long 50 Ω microstrip line printed on a 1 mm thick substrate with relative dielectric constant of $\varepsilon_r = 2.65$ is placed vertically inside the cell. Correspondingly, the incident angle θ in Fig. 1 is 0°, and the angle between the incident plane and XOZ plane ϕ is 90°.

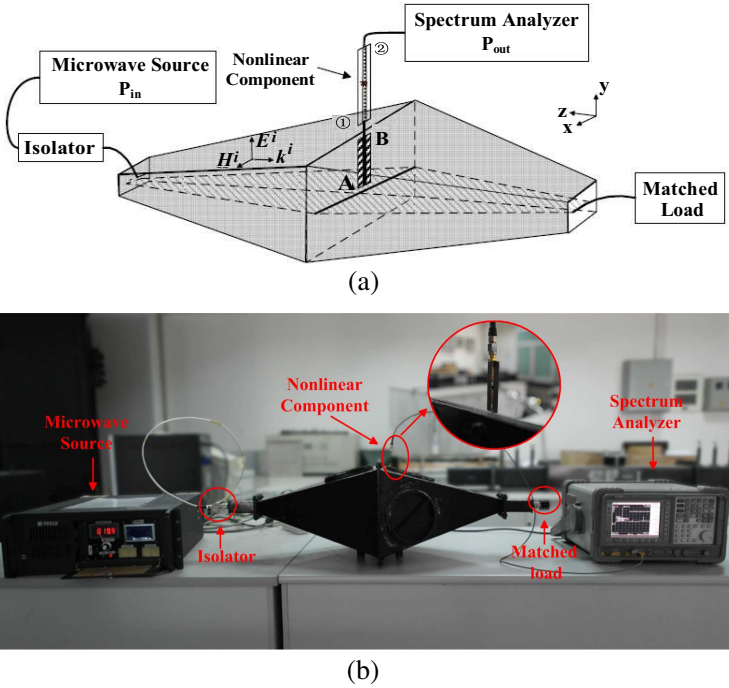

Figure 7. (a) Block diagram and (b) photograph of the whole validation system.

The microstrip line is terminated with a matched load at end A and connected to the nonlinear component (mentioned in Section 2) at the other end B (see Fig. 7). To make sure that only this ordinary microstrip line is illuminated by the electromagnetic field, the nonlinear component is placed outside the cell through a hole. The cell is excited by a microwave source, and the output power from the nonlinear component P_{out} is measured using a broadband spectrum analyzer.

First, the electromagnetic field coupling to the microstrip line connected to a matched load at the end B are computed using the field-to-TL coupling theory mentioned in Section 2. Fig. 8(a) shows an example of the voltage and current distribution along the line with the input power $P_{in} = 30\,\text{dBm}$. Here the field distribution inside the cell is obtained using FDTD method. Then the power transmitted to the load is calculated using these induced voltage and current. Fig. 8(b) displays the comparison between the calculated results and measured ones, and there is a good agreement between them. Obviously, the power coupled to the line increases linearly as the input power from the source rises.

Once the power transmitted to the load is obtained, the nonlinear

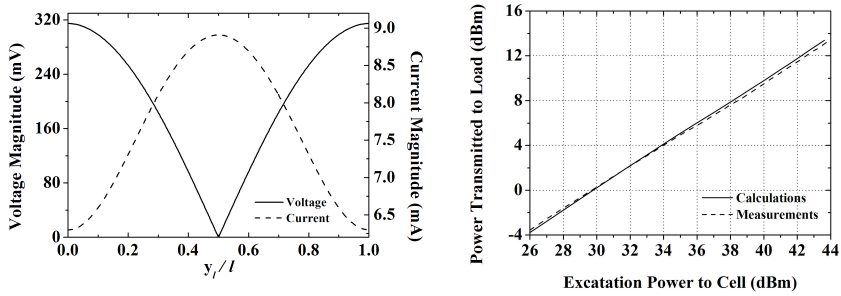

(a) (b)

Figure 8. Calculated results using field-to-TL coupling theory. (a) Magnitude of induced voltage and current along the line, and (b) power transmitted to the matched load.

S-parameters are used to get both fundamental and third harmonic output power P_{out} from the nonlinear component according to Eq. (4). Because the nonlinear component is connected to the broadband spectrum analyzer (namely, a matched load), there is no incident power at port ② at all. Consequently, Eq. (4) is simplified as the following Eq. (6), by which the reflected power at the port ① and transmitted power at the port ② can then be calculated.

$$\begin{bmatrix} b_1^1 \\ b_1^2 \\ b_1^3 \\ b_2^1 \\ b_2^2 \\ b_2^3 \end{bmatrix} = \begin{bmatrix} S_{11}^{11} & S_{11}^{12} & S_{11}^{13} & S_{12}^{11} & S_{12}^{12} & S_{12}^{13} \\ S_{11}^{21} & S_{11}^{22} & S_{11}^{23} & S_{12}^{21} & S_{12}^{22} & S_{12}^{23} \\ S_{11}^{31} & S_{11}^{32} & S_{11}^{33} & S_{12}^{31} & S_{12}^{32} & S_{12}^{33} \\ S_{21}^{11} & S_{21}^{12} & S_{21}^{13} & S_{22}^{11} & S_{22}^{12} & S_{22}^{13} \\ S_{21}^{21} & S_{21}^{22} & S_{21}^{23} & S_{22}^{21} & S_{22}^{22} & S_{22}^{23} \\ S_{21}^{31} & S_{21}^{32} & S_{21}^{33} & S_{22}^{31} & S_{22}^{32} & S_{22}^{33} \end{bmatrix} = \begin{bmatrix} a_1^1 \\ 0 \\ 0 \\ 0 \\ 0 \\ 0 \end{bmatrix} \tag{6}$$

The necessary four parameters in the dashed box have already been extracted through measurements and the rest two $|S_{11}^{21}|$ and $|S_{21}^{21}|$ are zero, since there is no second harmonic response at both ports, as mentioned in Section 2.

A question deserving more attention is that the induced voltage and current distribution highly depend on the incident electromagnetic wave and the loads at both ends of the TL. However, the equivalent impedance of the nonlinear component usually varies in terms of the power input to it, which results in the power transmitted to it changing accordingly. Therefore, the equivalent impedance Z_{eff} of the nonlinear component in terms of the input power is simulated using ADS, and results are shown in Fig. 9. The maximum transmitted power to matched load due to the induced voltage and current on the line is

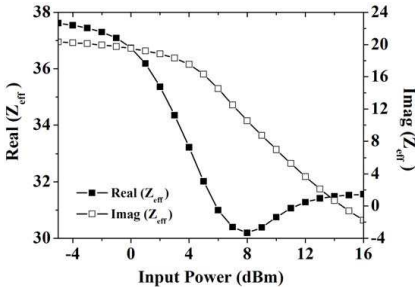

Figure 9. Equivalent impedance Z_{eff} of nonlinear component in terms of input power.

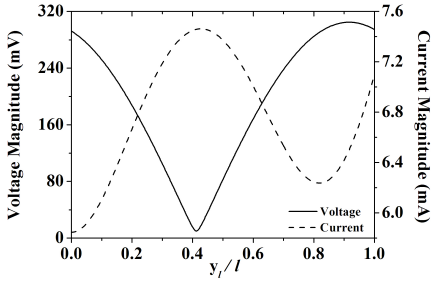

Figure 10. The magnitudes of the induced voltage (solid) and current (dashed) along the microstrip line connected with the nonlinear component.

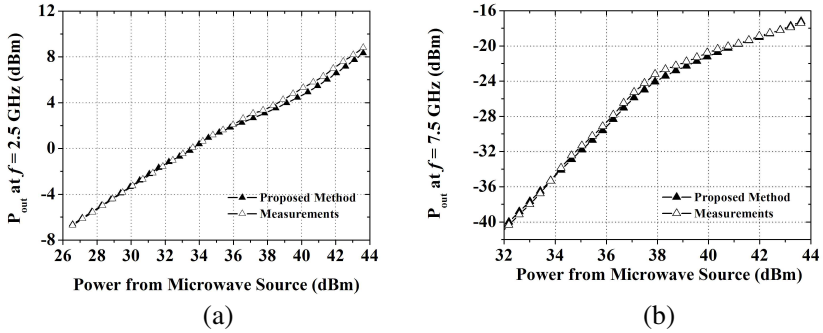

Figure 11. Comparison between the measured and predicted output power of (a) the fundamental and (b) the third harmonic components.

13.6 dBm (see Fig. 8(b)), so the maximum input power to the nonlinear component is set to be 16 dBm here.

Figure 10 presents the induced voltage and current distribution along the microstrip line calculated using the effective impedance, when the excitation power is the same as in Fig. 8(a). It can be observed that the voltage and current distribution is different much from that along the line terminated with a matched load.

Finally, the output power from the nonlinear component is predicted based on nonlinear S-parameters and the input power calculated using the induced voltage and current. Comparison between the measured results and predicted ones is shown in Fig. 11. The prediction agrees closely with the measurement, which demonstrates

the validation of the proposed method. Furthermore, the output power of both fundamental and third harmonic components varies nonlinearly as the input power from the microwave source rises.

It is noteworthy that electromagnetic wave is reflected from the nonlinear component back to the ordinary microstrip line, not only at the fundamental frequency, but also at the third harmonic. As mentioned previously, the ordinary microstrip line is terminated with a matched load at port A, and therefore the power of the reflected wave is absorbed. However, this reflected wave (especially the harmonic component) may cause other problems in a real electronic system.

4. CONCLUSIONS

An analysis method for electromagnetic field coupling to microstrip line connected with nonlinear components is proposed in this paper. The classical field-to-TL coupling theory (Taylor model) is used to get the response of a microstrip line illuminated by electromagnetic wave, while nonlinear components or devices are modeled by large-signal scattering parameters which are based on the black box model in frequency-domain. Then the electromagnetic field coupling to microstrip line connected with nonlinear components is analyzed by combining these two models together properly and considering the equivalent impedance of the nonlinear component. The predicted results using the proposed method are in good agreements with measured ones. Although the nonlinear component used in this paper is not a practical circuit like a mixer or low noise amplifier (LNA), the proposed method is appropriate for all the nonlinear devices or ICs, due to its basis on the black box model.

ACKNOWLEDGMENT

This work is supported by NSAF (Grant No. 11176017) and 973 Program (Grant No. 2013CB328904). The authors would like to thank the reviewers for their helpful comments in the preparation of the paper.

REFERENCES

1. Wu, Q., J.-H. Fu, and F.-Y. Meng, "A system-level EMC technical support platform for network-based computers," *2008 Asia-Pacific Symposium on Electromagnetic Compatibility & 19th International Zurich Symposium on Electromagnetic Compatibility*, 642–645, May 19–22, 2008.

2. Zamir, R., V. Bar-Natan, and E. Recht, "System level EMC — From theory to practice," *International Symposium on Electromagnetic Compatibility*, Vol. 3, 741–743, 2005.
3. Taylor, C. D., R. S. Satterwhite, and C. W. Harrison, Jr., "The response of a terminated two-wire transmission line excited by a nonuniform electromagnetic field," *IEEE Transactions on Antennas and Propagation*, Vol. 13, No. 6, 987–989, 1965.
4. Agrawal, A. K., H. J. Price, and S. H. Gurbaxani, "Transient response of multi-conductor transmission lines excited by a nonuniform electromagnetic field," *IEEE Transactions on Electromagnetic Compatibility*, Vol. 22, No. 2, 119–129, 1980.
5. Rachidi, F., "Formulation of the field-to-transmission line coupling equations in terms of magnetic excitation field," *IEEE Transactions on Electromagnetic Compatibility*, Vol. 35, No. 3, 404–407, 1993.
6. Rajkumar, E. R., B. Ravelo, M. Bensetti, and P. Fernandez-Lopez, "Application of a hybrid model for the susceptibility of arbitrary shape metallic wires disturbed by EM near-field radiated by electronic structures," *Progress In Electromagnetics Research B*, Vol. 37, 143–169, 2012.
7. Xie, Y.-Z., J. Guo, and F. G. Canavero, "Analytic iterative solution of electromagnetic pulse coupling to multiconductor transmission lines," *IEEE Transactions on Electromagnetic Compatibility*, Vol. PP, No. 99, 1–16, 2013.
8. Xie, H., J. Wang, R. Fan, and Y. Liu, "SPICE models for radiated and conducted susceptibility analyses of multiconductor shielded cables," *Progress In Electromagnetics Research*, Vol. 103, 241–257, 2010.
9. Xie, H., J. Wang, R. Fan, and Y. Liu, "Study of loss effect of transmission lines and validity of a SPICE model in electromagnetic topology," *Progress In Electromagnetics Research*, Vol. 90, 89–103, 2009.
10. Zou, J., T. B. Jin, W. W. Li, J. Lee, and S. Chang, "A Hermite interpolation model to accelerate the calculation of the horizontal electric field of a lightning channel along a transmission line," *IEEE Transactions on Electromagnetic Compatibility*, Vol. 55, No. 1, 124–131, 2013.
11. Manfredi, P. and F. G. Canavero, "Polynomial chaos for random field coupling to transmission lines," *IEEE Transactions on Electromagnetic Compatibility*, Vol. 54, No. 3, 677–680, 2012.
12. Poljak, D. and K. El Khamlichi Drissi, "Electromagnetic field coupling to over head wire configurations: Antenna model versus

transmission line approach," *International Journal of Antennas and Propagation*, Vol. 2012.

13. Magdowski, M. and R. Vick, "Closed-form formulas for the stochastic electromagnetic field coupling to a transmission line with arbitrary loads," *IEEE Transactions on Electromagnetic Compatibility*, Vol. 54, No. 5, 1147–1152, 2012.
14. Xie, H., J. Wang, S. Li, H. Qiao, and Y. Li, "Analysis and efficient estimation of random wire bundles excited by plane-wave fields," *Progress In Electromagnetics Research B*, Vol. 35, 167–185, 2011.
15. Mandic, T., R. Gillon, B. Nauwelaers, and A. Baric, "Characterizing the TEM cell electric and magnetic field coupling to PCB transmission lines," *IEEE Transactions on Electromagnetic Compatibility*, Vol. 54, No. 5, 976–985, 2012.
16. Archambeault, B., C. Brench, and S. Connor, "Review of printed-circuit-board level EMI/EMC issues and tools," *IEEE Transactions on Electromagnetic Compatibility*, Vol. 52, No. 2, 455–461, 2010.
17. Baum, C. E., "Extension of the BLT equation into time domain," *Interaction Note*, Vol. 553, 1999.
18. Tesche, F. M., "Development and use of the BLT equation in the time domain as applied to a coaxial cable," *IEEE Transactions on Electromagnetic Compatibility*, Vol. 49, No. 1, 3–11, 2007.
19. Xie, L. and Y. Z. Lei, "Transient response of a multiconductor transmission line with nonlinear terminations excited by an electric dipole," *IEEE Transactions on Electromagnetic Compatibility*, Vol. 51, No. 3, 805–810, 2009.
20. Tesche, F. M., "On the analysis of a transmission line with nonlinear terminations using the time-dependent BLT equation," *IEEE Transactions on Electromagnetic Compatibility*, Vol. 49, No. 2, 427–433, 2007.
21. Taeb, A., A. Abdipour, and A. Mohhamadi, "FDTD analysis of the lossy coupled transmission lines loaded by nonlinear devices," *Asia-Pacific Microwave Conference Proceedings*, Vol. 5, 2005.
22. Xie, H. Y., J. G. Wang, and R. Y. Fan, "A hybrid FDTD-SPICE method for transmission lines excited by a nonuniform incident wave," *IEEE Transactions on Electromagnetic Compatibility*, Vol. 51, No. 3, 811–817, 2009.
23. Paul, C. R., "A SPICE model for multiconductor transmission lines excited by an incident electromagnetic field," *IEEE Transactions on Electromagnetic Compatibility*, Vol. 36, No. 4, 342–354, 2009.

24. Bayram, Y. and J. L. Volakis, "Hybrid S-parameters for transmission line networks with linear/nonlinear load terminations subject to arbitrary excitations, " *IEEE Transactions on Microwave Theory and Techniques*, Vol. 55, No. 5, 941–950, 2007.
25. Root, D. E., J. Verspecht, D. Sharrit, J. Wood, and A. Cognata, "Broad-band poly-harmonic distortion (PHD) behavioral models from fast automated simulations and large-signal vectorial network measurements," *IEEE Transactions on Microwave Theory and Techniques*, Vol. 53, No. 11, 3656–3664, 2005.
26. Jargon, J., K. C. Gupta, and D. Schreurs, "A method of developing frequency-domain models for nonlinear circuits based on large-signal measurements," *58th ARFTG Conference Digest-Fall*, Vol. 40, 1–14, 2001.
27. Jargon, J. A., K. C. Gupta, and D. C. de Groot, "Nonlinear large-signal scattering parameters: Theory and application," *63rd ARFTG Microwave Measurement Conf. Dig.*, 157–174, 2004.
28. Rachidi, F. and S. Tkachenko, "Electromagnetic field interaction with transmission lines," Part I, Chapter 2, WIT Press, 2008.
29. Nucci, C. A. and F. Rachidi, "On the contribution of the electromagnetic field components in field-to-transmission lines interaction," *IEEE Transactions on Electromagnetic Compatibility*, Vol. 37, No. 4, 505–508, 1995.
30. Rachidi, F., "A review of field-to-transmission line coupling models with special emphasis to lightning-induced voltages on overhead lines," *IEEE Transactions on Electromagnetic Compatibility*, Vol. 54, No. 4, 898–911, 2012.
31. Bernardi, P. and R. Cicchetti, "Response of a planar microstrip line excited by an external electromagnetic field," *IEEE Transactions on Electromagnetic Compatibility*, Vol. 32, No. 2, 98–105, 1990.
32. Jeffrey, A. J. and D. C. de Groot, "Frequency-domain models for nonlinear microwave devices based on large-signal measurements," *Journal of Research of the National Institute of Standards and Technology*, Vol. 109, No. 4, 407–427, 2004.
33. Cohn, M., J. E. Degenford, and B. A. Newman, "Harmonic mixing with an anti-parallel diode pair," *IEEE Transaction on Microwave Theory and Techniques*, Vol. 23, No. 8, 667–673, 1975.